

Post-tsunami impact study on thermohaline structure in the Bay of Bengal

Alvarinho J. Luis*, S. M. Pednekar and M. Sudhakar

National Centre for Antarctic and Ocean Research, Headland Sada, Goa 403 804, India

Temperature and salinity profiles measured on-board *ORV Sagar Kanya*, during 18 January–17 February 2005, in the vicinity of the Chennai coast and west of the Andaman (AN) Islands, have been employed to assess and quantify the post-tsunami impact on the upper-ocean thermohaline structure, by comparing these with previous year's data. In the vicinity of the AN Islands, the sea surface temperature increased by 0.5°C and surface salinity decreased from 33.5 to 32 psu, between 90°E and 92°E along 10°N. This freshening has been attributed to westward geostrophic flow from the AN Sea facilitated by a sea surface height gradient inferred from the merged multi-mission satellite data. Significant temperature variations exceeding 1°C were observed between 50 and 250 m, west of the AN Islands. Near the Chennai coast (10°N, 80.9°E), influx of freshwater from the northern Bay of Bengal reduced salinity by 0.8 psu and stratification in the upper 100 m was observed. Upward shift in the 20°C isotherm was observed at all locations, suggesting a vertical entrainment. In general, this study reveals that considerable thermohaline variability has occurred in the upper 300 m water column, which is expected to have a significant impact on primary production and fisheries.

Keywords: Post-tsunami impact, temperature and salinity profiles, thermohaline structure.

THE largest seismic event on earth during the past 40 years ruptured a 1600 km-long portion of the fault boundary between the Indo-Australian and southeastern Eurasian plates on 26 December 2004. This earthquake, with its epicentre at 257 km south-southeast of Banda Aceh, Sumatra Island, Indonesia, released about 20×10^{17} J of energy¹, triggering a killer tsunami uncommon to the Indian Ocean region. It caused the death of over two lakh people and damaged property worth billions of dollars along the Indian Ocean-rim countries. These fast-gravity waves (or deep-water waves) have wavelength in excess of 100 km and a height of 0.3–0.6 m in the open ocean; they propagate with a speed of the order of 600–800 km/h and as they ingress onto the continental shelves, the frictional influence due to shoaling topography reduces their speed and increases the wave height to conserve the total energy. Hence at the coast these waves appear as a series of walls of breaking

waves. The height of the tsunami wave was reported to be 6 m at the Chennai coast about 2½ h after the Sumatra earthquake. So we expect modulations in the vertical water column in the vicinity of the continental shelf of India.

The National Centre for Antarctic and Ocean Research (NCAOR), Goa, undertook an oceanographic cruise on-board *ORV Sagar Kanya* to collect geophysical data in order to assess and quantify the impact of tsunami on the marine environment. With this aim, the conductivity–temperature–depth (CTD) observations² were made along 500 m isobath from Goa to Chennai (Leg-1) during 3–15 January 2005. Thereafter, the ship sailed from the Chennai port and headed towards eastern Bay of Bengal (BB). During this survey, geophysical and CTD measurements down to 1000 m were made along 10°N transect and in the vicinity of Andaman (AN) Islands³ during 18 January–17 February 2005 (Leg-2; Figure 1). Using these hydrographic data we quantify the thermohaline changes by comparing the temperature and salinity profiles (hereafter referred to as post-tsunami data) with profiles sampled during previous years (hereafter referred to as pre-tsunami data), which were available only at a very few locations (Table 1).

We utilized temperature and salinity profiles, which were collected south of Chennai (10°N, 80.9°E) and west of AN Islands (along 10°N at 90°E, 91°E and 92°E, and at 13.5°N, 91°E). These profiles were acquired using the SeaBird CTD system (SBE 9/11; accuracy, temperature $\pm 0.001^\circ\text{C}$, conductivity ± 0.0001 S/m and depth $\pm 0.005\%$ of full scale) at the geographic locations shown in Figure 1. Offsets in the salinity values were corrected with Autosol readings (Guild line, 8400A) using *in situ* samples collected at selected depths with Rosette samplers attached to the underwater CTD unit. The temperature and salinity profiles were recorded at 1° longitude interval and resolved at 1 m in the vertical.

Data have been quality-controlled following the protocol adopted by the National Oceanographic Data Centre,

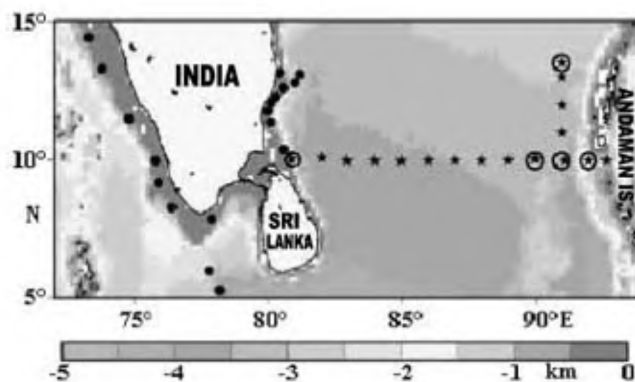


Figure 1. Topographic map of the study area superimposed with CTD stations occupied during the post-tsunami cruise. Stations indicated by solid dots (stars) were occupied during Leg-1 (Leg-2). CTD stations indicated by stars with open circles were used to quantify the post-tsunami impact addressed in this work.

*For correspondence. (e-mail: alvluis@ncaor.org)

Table 1. Comparison between pre- and post-tsunami upper-ocean hydrographic features. Mixed layer depth is defined as the depth where the density changed by 0.125 from the surface value⁶

Location	Mixed layer depth (m)		Depth of 20°C isotherm (m)	
	Pre-tsunami	Post-tsunami	Pre-tsunami	Post-tsunami
10°N, 80.9°E	18	23	125	108
10°N, 90°E	62	32	122	121
10°N, 91°E	75	55	134	119
10°N, 92°E	43	34	121	113
13.5°N, 91°E	46	31	128	123

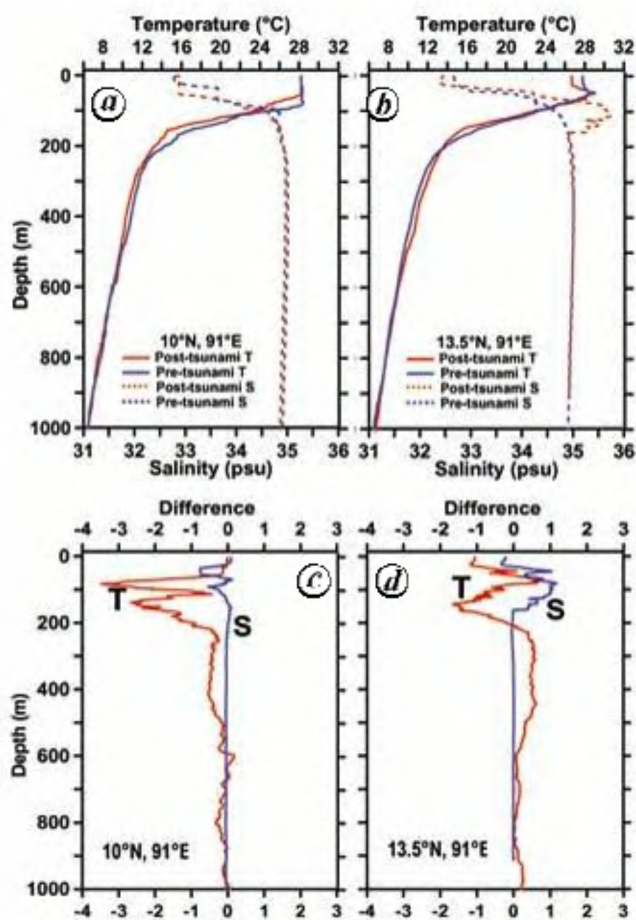


Figure 2. Vertical temperature and salinity profiles at (a) 10°N, 91°E and (b) 13.5°N, 91°E. Post-tsunami minus pre-tsunami temperature (*T*, °C) and salinity (*S*, psu) at (c) 10°N, 91°E and (d) 13.5°N, 91°E.

USA^{4,5}. Pre-tsunami data collected during January 2004 on-board *ORV Sagar Kanya* and two profiles (10°N, 80.9°E and 10°N, 92°E) obtained from the archives of the World Ocean Database (<http://www.nodc.noaa.gov>) for January 1972 have been employed for comparison. These pre-tsunami data have been collocated with post-tsunami data with a time difference of utmost a month and a spatial distance of 25 km. Using the pre- and post-tsunami profiles we have monitored the depth of the 20°C isotherm to infer changes at the mid-thermocline and quantified the

mixed layer depth (MLD), which is defined as the depth where the density changes by 0.125 from the surface value⁶ (Table 1).

Additionally, geostrophic currents derived from multi-mission (Jason-1, Topex/Poseidon, ERS-2 and Envisat) sea surface height anomalies, which were computed with respect to the seven-year mean (1992–99), have been employed. These were computed using centred finite difference method at weekly intervals with a spatial resolution of $1/3^\circ \times 1/3^\circ$ (<http://www.aviso.oceanobs.com/>). The geostrophic currents were mapped to understand the modulation of flow through the 10°N channel prior to and after the tsunami.

Now we highlight the modulations in temperature and salinity due to the tsunami by comparing the post-tsunami data with the pre-tsunami profiles. Locations of these profiles are indicated by a star with an open circle in Figure 1 and their geographical position is given in Table 1. Figure 2 depicts vertical profiles of temperature and salinity observed at 10°N and 13.5°N along 91°E; the red (blue) profiles denote post-tsunami (pre-tsunami) data. At 10°N, 91°E, the post-tsunami profile indicated no appreciable change in surface temperature and salinity (Figure 2a). However, the mixed layer thickness was reduced from 75 to 55 m and the 20°C isotherm shallowed by 15 m (Table 1). The latter resulted in a temperature difference (post-minus pre-tsunami) exceeding 1°C between 80 and 200 m (Figure 2c). A salinity difference of 0.8 and 0.5 psu at 50 and 100 m respectively, was observed (Figure 2c). In brief, Figure 2a and c suggests that highest cooling occurred between 50 and 200 m and salinity decreased in the upper 100 m.

Moving northward to 13.5°N, 91°E, it was observed that the sea surface temperature (SST) decreased by 1.2°C compared to the pre-tsunami profile (Figure 2b). Though a temperature inversion was identified in the pre- and post-tsunami profiles at 40 m, temperature was subdued by 1°C in the post-tsunami case (Figure 2b). The 20°C isotherm had shifted upward by 5 m (Table 1) and a temperature cooling of 1.8°C was observed at 150 m (Figure 2d). The salinity profile revealed a decrease in surface salinity by 0.3 psu and an increase in the halocline gradient from 0.0166 to 0.5841 psu/m, which resulted in a positive salinity difference of 1 psu at 75 m (Figure 2d). A subsurface salinity maximum of 35.7 psu was encoun-

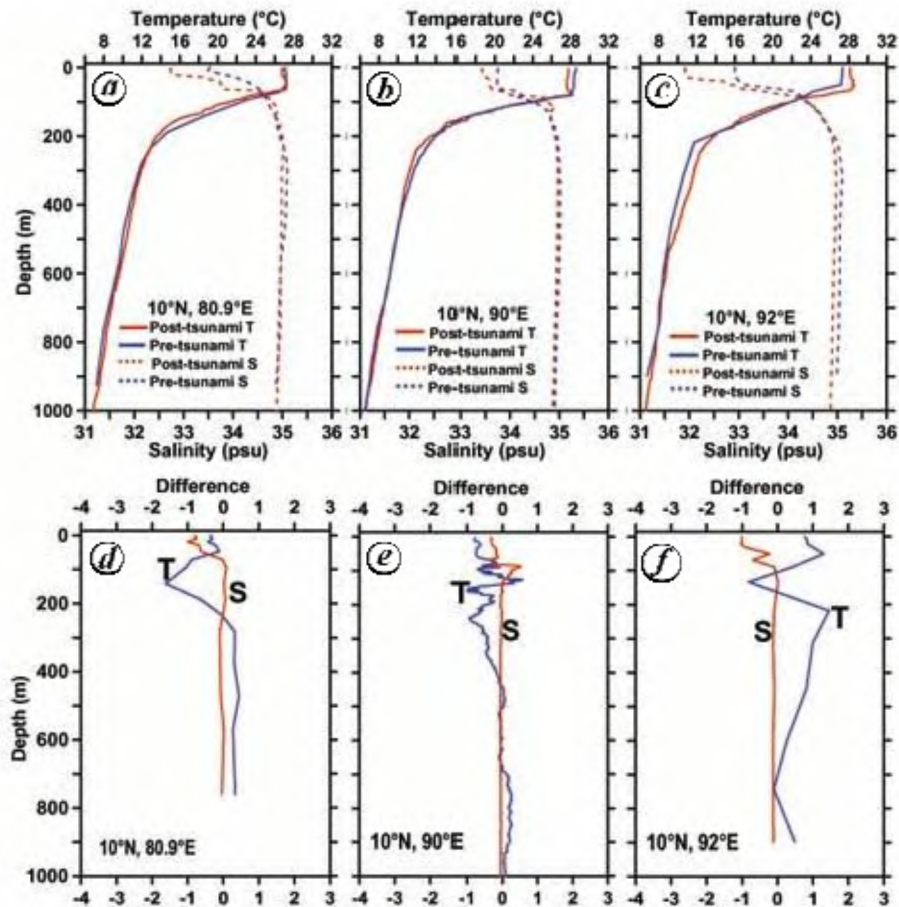


Figure 3. Vertical temperature and salinity profiles at (a) 10°N , 80.9°E , (b) 10°N , 90°E and (c) 10°N , 92°E . Post-tsunami minus pre-tsunami temperature (T , $^{\circ}\text{C}$) and salinity (S , psu) at (d) 10°N , 80.9°E , (e) 10°N , 90°E and (f) 10°N , 92°E .

tered at 120 m, which was absent in the pre-tsunami profile. In brief, the analysis of thermohaline structure at 13.5°N , 91°E indicated that (i) the MLD decreased by 15 m and the temperature cooled by 1.8°C at 150 m; (ii) the halocline gradient increased by 34% and a prominent subsurface salinity maximum occurred at 120 m. In summary, along 91°E analysis of the post-tsunami scenario revealed a decrease in SST by 1.7°C between 10°N and 13.5°N , and a temperature inversion at 40 m and salinity maximum at 120 m at the northern location.

Now we highlight the thermohaline changes along 10°N (Figure 3). At 10°N , 80.9°E , which is off the Chennai coast where the depth is about 1000 m, the post-tsunami temperature profile showed a marginal decrease of 0.5°C in SST (Figure 3 a), an increase in the MLD from 18 to 23 m (Table 1) and an upward shift of the 20°C isotherm by 17 m (Table 1). The latter feature caused a fall in post-tsunami temperature by 1.8°C at 150 m (Figure 3 d). The post-tsunami salinity profile revealed a decrease in surface salinity from 33.5 to 32.7 psu (Figure 3 a) and a stratification in the upper 80 m (Figure 3 d). Moving

eastward to 10°N , 90°E , the post-tsunami temperature profile depicted an isothermal layer cooled by 0.8°C and a weak temperature inversion at 90 m, compared with the pre-tsunami (Figure 3 b). On the other hand, in the post-tsunami profile the surface salinity decreased by 0.4 psu and the halocline extended to near surface, compared to the pre-tsunami profile. Salinity changes were confined to the upper 120 m, while the temperature change of less than a degree occurred in the upper 250 m (Figure 3 e). The MLD thickness shallowed by 50% (Table 1).

Moving closer to the AN Islands, at 10°N , 92°E the post-tsunami temperature profile showed an increase in SST by 0.8°C and a subsurface temperature inversion at 75 m, which was absent in the pre-tsunami profile (Figure 3 c). The salinity decreased by 1 and 0.2 psu at the surface and below 250 m, respectively, from the pre-tsunami value (Figure 3 c). The 20°C isotherm was uplifted by 8 m, while the MLD was reduced by 9 m (Table 1). The post-tsunami changes were quantified as follows (Figure 3 f): (i) The temperature increased by 1.2°C at 50 m and fell by a degree near 150 m. (ii) Maximum decrease in sali-

nity by 1 psu occurred at the surface. The marginal temperature difference of $<0.6^{\circ}\text{C}$ below 220 m was attributed to a poor depth resolution in the pre-tsunami profile.

In brief, in the post-tsunami scenario it was found that surface cooling of 0.5°C and a decrease in the surface salinity by 0.8 psu occurred near the Chennai coast, while SST increased by 0.8°C and surface salinity dropped by 1 psu, west of the AN islands. Pronounced cooling of 1.8°C at 150 m and a 16 m upward shift of the 20°C isotherm occurred near Chennai, compared to 1°C dip at 150 and 8 m upward shift of the 20°C isotherm, west of the AN Islands.

From the preceding results we can summarize the significant findings and identify the plausible mechanisms for the observed changes. At the location closer to the 10°N channel (10°N , 92°E), the surface salinity dropped by 1 psu; the MLD was reduced by 9 m and the 20°C isotherm shifted upward by 8 m (Figure 3 c). At 10°N , 91°E , which is about 110 km west from the preceding station, SST and surface salinity showed no change (Figure 2 a), but MLD increased by 30 m and the 20°C isotherm moved up by 15 m (Table 1). Moving further west to 10°N , 90°E , we observed a 0.5°C dip in SST, a decrease of 0.3 psu in the surface salinity and thinning of MLD by 30 m (Figure 3 b and Table 1). From these observations we note that the SST increased by 0.5°C and the surface salinity decreased from 33.5 to 32 psu, between 90°E and 92°E . Though a decreasing trend in salinity of 0.3 psu has been reported in the climatological world ocean atlas⁴, the change observed in the present work was much higher (1.5 psu).

To explain the large salinity variation, we examined salinity profiles collected from the AN Sea. These showed a surface salinity of <33 psu (also see figure 39 c in Varkey *et al.*⁷) and SST of $\sim 28^{\circ}\text{C}$. So we suggest that the water has drifted from the AN Sea to the BB through the 10°N channel after the tsunami. This was possible because the sea surface height anomaly for first week of January 2005, inferred from the merged multi-mission satellite altimeter data, was 15 cm in the AN Sea compared to 5 cm to the west of the channel; this sea surface gradient permitted such a drift. The possibility that this water drifted from the Equatorial Indian Ocean (EIO) was remote, because the surface salinity of the EIO water exceeded 33 psu.

To further strengthen the above inference, we constructed maps of geostrophic currents derived from merged sea surface height anomalies for the pre-tsunami (25 December 2004) and post-tsunami period (1 January 2005; Figure 4). It is inferred that geostrophic flow through the 10°N channel prior to the tsunami was disorganized and weak (<0.1 m/s). It also shows an anticyclonic circulation in the AN Sea, which has been reported in the literature⁷ during boreal winter (Figure 4 a). However, in the post-tsunami scenario the anticyclonic circulation in the AN Sea was strengthened and a part of this flow entered the BB through the 10°N channel (Figure 4 b). So it is clear

that the southern limb of the anticyclonic circulation transported the low saline water from the AN Sea, which lowered the salinity between 90°E and 92°E .

At the northern station (13.5°N , 91°E) surface salinity dropped by 0.3 psu and a subsurface salinity maximum (35.7 psu) at 120 m was identified. We also found similar salinity maximum at 10°N , 84°E . No explanation can be offered for the source of this subsurface high salinity water because existence of such high salinity water was unknown to the BB. However, the Arabian Sea (AS) high salinity water, with a salinity range of 34.6–35.2 psu has been reported in the central BB, which was advected from the AS to the southwestern BB at subsurface depths of 75–100 m by the equatorward flowing West India Coastal Current during boreal summer⁸. The decrease in salinity in the upper 100 m at 10°N , 80.9°E could be attributed to

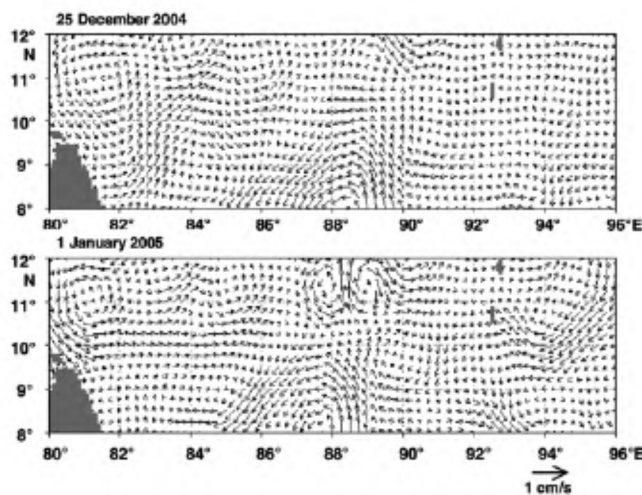


Figure 4. Geostrophic currents (u, v) derived from merged multi-mission gridded sea surface height anomalies (η) computed with respect to seven-year mean (1992–99), using spatial gradients of η : $v = (g/f)/(\partial\eta/\partial x)$, $u = -(g/f)/(\partial\eta/\partial y)$, where g is acceleration due to gravity (ms^{-2}) and f the Coriolis force (s^{-1}). Note a strong westward flow from Andaman Sea after the tsunami (lower panel).

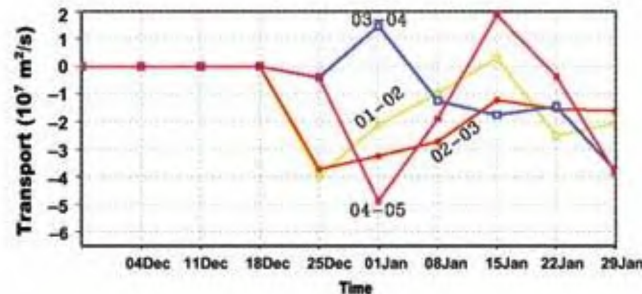


Figure 5. Geostrophic transport ($10^7 \text{ m}^2/\text{s}$) integrated from 9°N to 11°N along 93°E during December–January for different years. Geostrophic currents at weekly intervals were estimated from multi-mission gridded sea surface height anomalies computed with respect to seven-year mean (1992–99). Note the enhanced westward transport immediately after the tsunami (26 December 2004). Negative ordinate indicates a westward transport.

the transport of freshwater equatorward from the head BB by the wind-driven East India Coastal Current during the winter monsoon⁹.

In conclusion, analysis of temperature and salinity profiles collected during the post-tsunami period provided a wealth of information, which suggested that the thermohaline structure in the eastern BB was modulated by a drift of low saline water from the AN Sea. The influx of freshwater from the northern BB reduced surface salinity by 0.8 psu and stratification was observed in the vicinity of the Chennai coast. West of the AN Islands, SST increased by 0.8°C and significant temperature variations above 250 m were observed. An upward shift of the 20°C isotherm was observed at all locations, suggesting vertical entrainment. Modulations in the hydrographic properties were expected to have a strong impact on the flora and fauna in the vicinity of the AN Islands.

1. Rao, N. P. and Chary, A. H., What caused the great Sumatran earthquakes of 26 December 2004 and 28 March 2005? *Curr. Sci.*, 2004, **89**, 449–452.
2. Anilkumar, N., Sarma, Y. V. B., Babu, K. N., Sudhakar, M. and Pandey, P. C., Post-tsunami oceanographic conditions in southern Arabian Sea and Bay of Bengal. *Curr. Sci.*, 2006, **90**, 421–427.
3. Murthy, K. S. R., First oceanographic expedition to survey the impact of the Sumatra earthquake and the tsunami of 26 December 2004. *Curr. Sci.*, 2005, **88**, 1038–1039.
4. Levitus, S., Burgett, R. and Boyer, T. P., *NOAA Atlas NESDIS 3, World Ocean Atlas 1994, Volume 3, Salinity*, National Oceanographic Data Center, Ocean Climate Laboratory, Washington DC, USA, p. 99.
5. Levitus, S. and Boyer, T. P., *NOAA Atlas NESDIS 4, World Ocean Atlas 1994, Volume 3, Temperature*, National Oceanographic Data Center, Ocean Climate Laboratory, Washington DC, USA, p. 117.
6. Morrison, J. M., Codispoti, L. A., Gaurin, S., Jones, B., Manghnani, V. and Zheng, Z., Seasonal variation of hydrographic and nutrient fields during the US JGOFS Arabian Sea process study. *Deep Sea Res. II*, 1998, **45**, 2053–2101.
7. Varkey, M. J., Murty, V. S. N. and Suryanarayana, A., Physical oceanography of the Bay of Bengal and Andaman Sea. In *Oceanography and Marine Biology: An Annual Review* (eds Ansell, A. D., Gibson, R. N. and Barnes, M.), UCL Press, London, UK, 1996, vol. 34, pp. 1–70.
8. Murty, V. S. N., Sarma, Y. V. B., Rao, D. P. and Murty, C. S., Water characteristics, mixing and circulation in the Bay of Bengal during southwest monsoon. *J. Mar. Res.*, 1992, **50**, 207–228.
9. Shetye, S. R. *et al.*, Hydrography and circulation in the western Bay of Bengal during the northeast monsoon. *J. Geophys. Res.*, 1996, **101**, 14011–14026.

ACKNOWLEDGEMENTS. We thank Dr R. Ravindra, Director, NCAOR, for encouragement and interest in this work and Ministry of Earth Sciences (formerly DOD), New Delhi for financial support. We also thank the Director, Central Marine Living Resources and Ecology, Cochin, for providing pre-tsunami data. Altimeter products were produced by Ssalto/Duacs and distributed by AVISO, with support from Centre National d'études Spatiales. We acknowledge the cooperation of the Master and participants of *ORV Sagar Kanya* cruise-217. Constructive comments from the reviewers helped in improving the manuscript.

Received 2 December 2005; revised accepted 12 June 2007

Sea-water pH and planktic foraminiferal abundance: Preliminary observations from the western Indian Ocean

R. Saraswat^{1,2,*}, N. Khare¹, S. K. Chaturvedi¹ and A. Rajakumar¹

¹National Centre for Antarctic and Ocean Research, Headland Sada, Vasco-da-Gama, Goa 403 804, India

²Present address: Centre for Advance Studies in Geology, Department of Geology, University of Delhi, Delhi 110 007, India

The planktic foraminiferal abundance has been calculated in a set of 28 surface sediment samples collected from the equatorial and southwestern Indian Ocean. In order to understand the influence of changing sea-water pH on the planktic foraminiferal abundance, the latter has been compared with average sea-water pH of the top 500 m of the water column, measured *in situ*. Though water depth shows a marked influence on the planktic foraminiferal abundance, pH also appears to affect the overall abundance of planktic foraminifera. The preliminary results indicate that the planktic foraminiferal abundance is directly proportional to sea-water pH.

Keywords: Abundance, pH, planktic foraminifera, sea-water, water depth.

VARIOUS physico-chemical and biological parameters control the foraminiferal abundance. Besides temperature and salinity, isotopic composition of the foraminiferal shells has also been shown to vary under changing carbonate ion concentration of the sea water as well as pH¹. The close relationship between sea-water pH and ocean carbon reservoir, lead to the development of foraminiferal proxies, to infer sea-water pH during geologic past. The boron isotopic composition of the selected foraminiferal species has been developed as an efficient proxy to infer past sea-water pH^{2,3}. Based on the laboratory and field-based studies, significant influence of sea-water pH on the boron isotopic composition of the foraminiferal shells has already been established⁴. Additionally, the shells of few foraminiferal species have been shown to dissolve under reduced pH conditions in laboratory culture studies⁵. The dissolution of foraminiferal tests as a result of change in pH with changing salinity has been proposed to affect the abundance of foraminiferal species as well^{5,6}.

Nevertheless, studies dealing with the effect of changing sea-water pH on the dissolution of the foraminiferal shells are limited. Therefore, in the present study we explore the possible influence of changing sea-water pH on the foraminiferal abundance in a set of samples collected along a

*For correspondence. (e-mail: rs.niog@gmail.com)